Mechanical characteristics, morphology and corrosion behavior of duplex stainless steel 2205

Amol Chaudhari[1], Nilesh Diwakar[2] and Shyamkumar Kalpande[3]

[1]*Ph.D. Research Scholar, SRK University, Bhopal, India.*
[2]*Prof. Department of Mechanical, SRK University, Bhopal, India.*
[3]*Prof. Department of Mechanical Engineering, GCOERC, Nashik, India*

camol1983@gmail.com, nileshdiwakar@gmail.com, shyamkalpande@gmail.com

Abstract:

Duplex stainless steel, also known as austenitic-ferritic stainless steel, is a high-performance material with superior mechanical and corrosion qualities that is commonly found in marine applications. Corrosion and mechanical performance degradation are common in the marine industry due to the demanding operating conditions at varying temperatures. The mechanical characteristics, morphology, and electrochemical behavior of 2205 duplex stainless steel at elevated processing temperatures in different cooling mediums are discussed in this paper. Optical and scanning electron microscopy (SEM) along with potentiodynamic tafel plots in water containing 3.5% NaCl solutions were used to examine the precipitation of distinct phases without and with heat treatment, as well as their impact on corrosion resistance. When comparing the mechanical properties of duplex stainless steels, air quenching was shown to produce the highest impact strength and average hardness values. Because of the greater volumetric precipitation of austenite after water cooling, the water-cooled sample performed better in corrosion resistance tests.

Keywords*:* DSS 2205, Toughness, Micro hardness, Morphology, corrosion, potentiodynamic Tafel.

1. Introduction

The name duplex stainless steel comes from the fact that the duplex structure of austenitic ferritic stainless steels precipitates in nearly equal volume fractions, resulting in excellent mechanical and corrosion properties. Duplex stainless steel (DSS) is becoming more popular for the fabrication of stainless-steel parts used in the maritime, chemical, oil and gas production, and pipeline sectors [1, 2]. Due to its high corrosion resistance, austenitic stainless steel is the most often used steel [3]. The percentages of Cr and Ni in DSSs are 18-28 and 4.5-8, respectively, and these are the principal alloying elements of DSSs [2]. The stability of austenite is managed by varying the percentages of Nitrogen, Carbon, Manganese, and other alloying elements such that particle and grain boundaries change, resulting in improvements in material properties like as strength and elongation [4-6]. To increase mechanical qualities and corrosion resistance, main, intermetallic phases, and alloying elements must be developed and partitioned [7]. The morphology of DSS demonstrates that the growth of the ferrite structure, which aids in the material's transition from ductile to brittle and lowers impact resistance, is directly connected to the existence of a ferritic phase [8]. However, the austenitic phase's emergence in the morphology enhanced the impact characteristics of DSS, allowing for permanent deformation and stopping the ferritic phase's low-energy brittle fracture [5-7]. In order to understand their mechanical properties, the quantity of intermetallic phases is crucial [6, 8, 9].

2. Literature Review

From the work done by the researchers, the percentages of the phases -ferrite, -austenite, and secondary phases like sigma and chi fluctuate with temperature in DSS, and the morphology changes with increased ferrite, decreased Ni content, and increased Cr content above recrystallization temperatures [10]. When Cr, Mo, and S-silicon are present, the stable elements in ferrite increase the tendency for secondary phases like sigma phase to develop. Important components for austenite production in the morphology of the DSS include nickel (Ni) and nitrogen (N) [7, 11]. The production of secondary phases such, 1 and 2 after cooling, however, compromises the material's mechanical characteristics and corrosion resistance at temperatures between 600°C and 900°C [10, 12, 13]. Sigma-, the most prevalent secondary phase, with concentrations as little as 0.05% significantly reduced the resistance to cracking during impact tests [8, 14]. The most appropriate heat treatment and cooling rate that aided in the creation of equilibrium phases that increased mechanical properties [15-17]. When the sample was heat treated at high temperatures (1000 to 1250°C) and swiftly cooled, the percentage volume of ferrite gradually increased while the percentage volume of austenite decreased [18-20]. The effect of heat treatment on duplex stainless steels resistance to pitting corrosion was also studied [19]. Kalyankar et al. [20] have looked into the potential failure of thin protective films made of duplex stainless steels in a 0.5 M NaCl water contain solution at different temperatures. Deshmukh et.al. [21] Investigated DSS's pitting and spontaneous creation of an ultra-thin film behavior in 1 M NaCl solution.

The effect of molybdate on the significant pitting temperature of duplex stainless steel in 0.1 M NaCl solution has also been explored by Deshmukh et.al [21]. Chaudhari et al. [22] reveal the behavior of super duplex stainless steel after sulfur addition on pitting corrosion and machine operation ability [23]. However, the environment to which stainless steel is exposed during vacuum desalination operations of salt and sea water has drawn the attention of several researchers. In the current experiments, the use potentiodynamic polarization and morphology analysis to compared the mechanical properties of duplex stainless steel 2205 before and after heat treatment at 1050^{o}C with different quenching environments, as well as its resistance to corrosion in water with NaCl solutions.

3. Methods

3.1 Material and mechanical properties

The square bar of Duplex stainless steel 2205 (10 x 10) utilized in the study has the chemical composition shown in Table 1 for its percentages of individual components. As can be seen in Fig. 1, a variety of notches were cut into standard 10 by 10 by 55 mm3 specimens in preparation for the charpy impact test. In order to prepare samples for mechanical testing, a wire cut electric discharge machine was used. The influence of high temperature treatment on microstructure, toughness, and corrosion behavior was studied using three different quenching environments: water, air, and furnace quenching to ambient temperature for treated specimens at 1050^{o}C, holding period 30 min. Table 2 displays the heating and cooling conditions utilized for specimens with various notches. At room temperature, the charpy test for mechanical toughness can be performed with an accuracy of 1 J using a maximum power of 300 J. A micro hardness measurement with a 1 kg weight is possible with a Vickers hardness tester.

3.2 Morphology analysis

The goal of morphology is to analyze and make sense of the DSS's structural shifts. In accordance with ASTM (E3-01) guidelines, the specimens are made ready for morphological analysis. Cutting, mounting, and wet-sanding with a variety of silicon carbide sheets to achieve a mirror sheen are just a few of the tasks involved in preparing a specimen for study. Murakami's reagent - Immersion etchant was used to prepare metallographic samples for the assessment of microstructural changes using an optical microscope, and the resulting mirror-like surfaces were then used to learn about particles and grain boundaries. Surface morphological features can be identified with the aid of a scanning electron microscope (SEM), and the microstructural appearances associated with austenite, ferrite, and secondary phases can be clearly illustrated. For SEM examination, a particular electrolytic etching procedure was applied, with 40% vol. HNO_3.

3.3 Electrochemical corrosion measurements

For the electrochemical tests, a standard three-electrochemical cell was used, with platinum serving as the counter electrode, a saturated calomel electrode (SCE) serving as the reference electrode, and duplex stainless steel 2205 functioning as the electrode. The specimens had a 10 mm x 15 mm footprint and a 3 mm depth. All four specimens were ground with silicon carbide paper and polished before testing, after heat treatment. A stream of air was utilized to dry the specimens after they were cleaned with ethyl alcohol. Measurement of corrosion rates with a GRAMY potantiostat. Before testing, the open circuit potential (OCP) is stabilized by dipping the working electrode into a 3.5% NaCl solution at ambient temperature to mimic the conditions of a seawater application.

Table 1. Chemical composition of 2205 DSS alloys (wt%)

Elements	**Cr**	**Ni**	**Mo**	**C**	**N**	**Mn**	**Fe**
Content	22.37 %	5.48%	3.49%	0.021%	0.20%	1.370%	Balance

Table 2. Notch samples with heating and quenching environment

Samples	**Temperature**	**Notches**	**Quenching Environment**
A1, B1, C1	1050 ℃	V, U and keyway	Untreated
A2, B2, C2	1050 ℃	V, U and keyway	Air quenching to atmospheric temperature
A3, B3, C3	1050 ℃	V, U and keyway	Water quenching to atmospheric temperature
A4, B4, C4	1050 ℃	V, U and keyway	Furnace quenching to atmospheric temperature

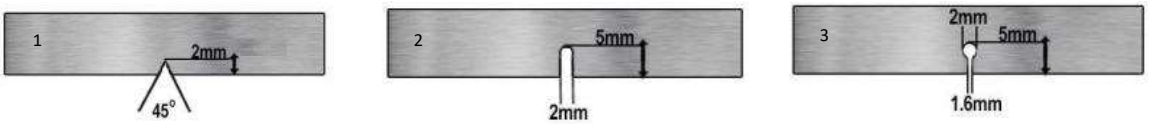

Fig. 1 Schematic diagram of the specimen for charpy impact test

4. Results

The untreated samples A1, B1, and C1 are depicted in Fig. 2 (1), and their morphologies reveal the absence of any intermetallic phases. The ferrite and austenite phases in these samples have volume fractions of 50.5% and 49.5%, respectively. In the morphology of the material revels that, the ferrite phase is characterized by a darker hue than the austenite phase there is no precipitation of secondary phase in all the specimens as shown in the Fig. 2. From the SEM morphology it was found that the ratio of percentage volume of ferrite and austenite was increases in the air- and water-cooled specimens and which is beneficial for the improvement in the mechanical properties. Several factors, including element, temperature range, and cooling time, affect the structure and amount of the secondary phase fraction. The corrosion resistance and mechanical properties of a material can be altered by the formation of secondary phases during heat treatment [5, 13]. If DSS 2205 is treated below the recrystallization temperature [7, 11, 19], the thermochemical equilibrium of phases is disrupted, leading to the precipitation of secondary phases via a thermodynamically stable state. Below 900 °C, the sigma phase could form [15]. During the investigation of mechanical property, results of charpy impact toughness indicate that, in air cooled specimens the percentage of austenite enhance up to 52-55% which improve the toughness of the specimen up to 33 J which is more than the other cooled medium. The SEM morphology of plane and furnace cooled specimen is nearly same as shown in Fig. 2 (1) and Fig. 2 (4). Maximum micro hardness obtained in the rapid cooled specimen as shown in the Table 4. There is no significant effect on the micro hardness, in all the specimens due to the absence of the intermetallic phases in the microstructure of the specimens which is beneficial for enhance the hardness. The instability of the ferrite phase above the recrystallization temperature causes it to react as ferrite-/austenite- or ferrite-/ferrite- interfaces, leading to secondary phases that are distinct from each other in microstructure and distributional organization. The result of three electrode corrosion test, the current density drops from 3.45 to 0.80 A/cm2 and maximum corrosion rate up to 1.589 mpy observed in furnace cooled and minimum corrosion rate up to 0.360 mpy water cooled specimen.

5. Discussion

5.1 Metallographic distribution of phases

SEM was used to investigate the effect of the heat treatment procedure on the central phase of the microstructure of the specimens. DSS specimens with and without 1050°C heat treatment using different quenching medium are shown in Fig. 2. Fig. 2 shows that the island-like austenite (γ) phase is not surrounded by a continuous matrix of ferrite (α) phase, as observed in several of the examined samples. Fig. 2 shows the SEM morphology of samples that were subjected to air quenching, water quenching, and furnace quenching to AT 1050°C for 30 minutes. Maximum diffusion rates of soluble alloys cause ferrite to be imbalanced in DSS's primary temperature range (600 °C - 900 °C), and enriching ferrite with Cr and Mo significantly degrades mechanical characteristics and forms secondary phases [4, 8, 15]. At temperatures above 900 degrees Celsius, -ferrite recrystallizes into a sigma- phase rather than austenite [13]. The volume fraction of the ferrite phase after heat treatment at 1050°C, air quenching, and water quenching to AT cooling is shown to be 52-54% and 52-55%, respectively, in Figures 2(2) and 2(3).

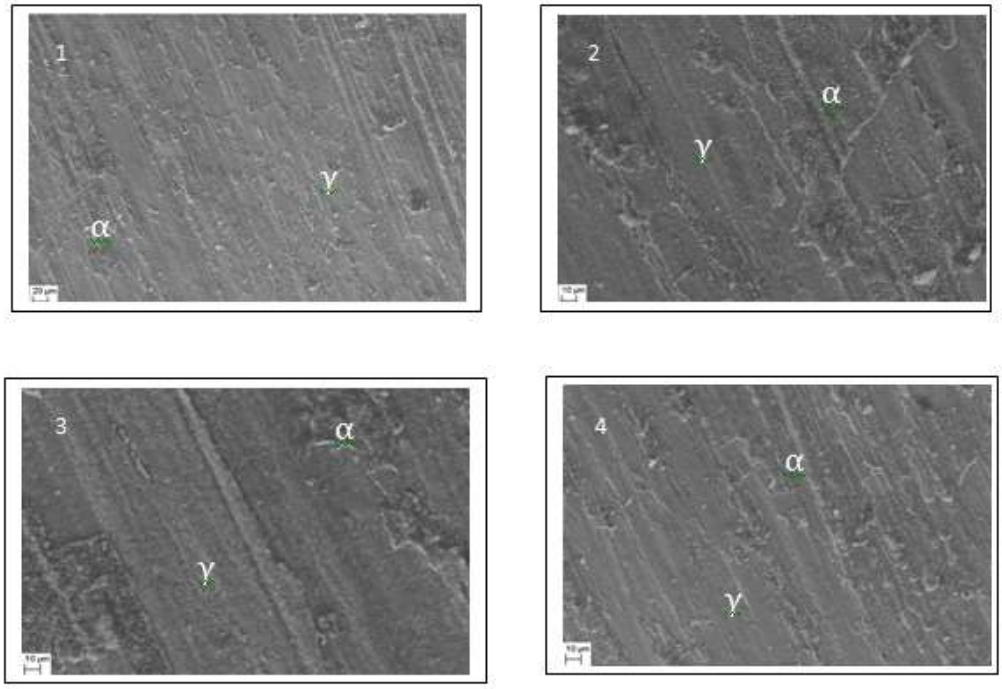

Fig 2. SEM image of the microstructure of (1) Untreated specimen, (2) air cooled specimen, (3) water cooled specimen and (4) furnace cooled specimen

5.2 Impact Toughness:

Some of the mechanical properties' relationships were determined after extensive research into heat treatment. Notched specimens were subjected to a dynamic test known as the Charpy toughness test, in which they were struck and broken down by a swinging pendulum. Three representative notches, each measuring 55 X 10 X 10 mm, will serve as test specimens. The quenching environment, heat treatment temperature, and untreated specimens are all listed in Table 2. Table 3 displays the amount of energy taken in by the notches in various conditions. The untreated specimen with the U and keyway notch had the lowest impact toughness, at 23 J. The morphology of untreated specimens with 49.5% volume in -ferrite and 51.5% volume in -austenite is depicted in Fig. 3(1). Rapidly cooled samples had a slightly higher volume % of austenite compared to the untreated sample. As can be shown in Fig. 3, the V notch sample A2 which was air quenched to atmospheric temperature (AT) had the highest value of toughness, i.e., 33 J, among the heat-treated specimens. This is because the austenite's volume fraction was enhanced to close to 52-55% after normalizing, and its fine-grained crystal structure resulted from the slow cooling. It has been shown that the presence of Cr and N elements in fast quench samples significantly reduces toughness in a variety of notches [7, 9, 14, 15]. Toughness values are revealed in Fig. 3 to be highest for air-cooled notch specimens and lowest for untreated specimens and those quenched in water. The results of this study showed that the toughness of the specimens in all of the notches was improved by high temperature heat treatment and quenching duration while avoiding the secondary phases.

Table 3. Toughness of notches for different quenching medium

Cooling medium	**Untreated**		**Air Quenching**		**Water Quenching**		**Furnace Quenching**	
Notches	Sample	Toughness (J)	Sample	Toughness (J)	Sample	Toughness (J)	Sample	Toughness (J)
V Notch	A1	24	A2	33	A3	27	A4	25
U Notch	B1	23	B2	31	B3	28	B4	24
Keyway Notch	C1	23	C2	30	C3	26	C4	23

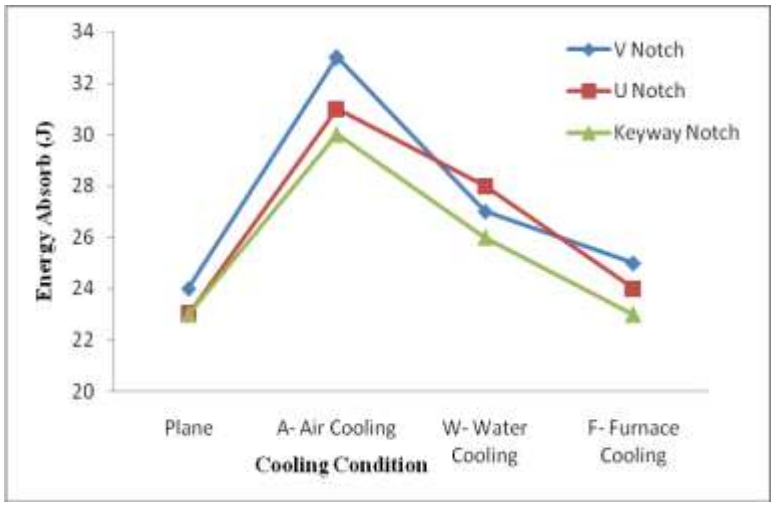

Fig. 3 Energy absorbed with different notch

5.3 Micro hardness:

The hardness of each of the three specimens was determined by examining them; the findings of the experiments suggest that the morphology of DSS contains both -ferrite and -austenite phases. The effects of applying a heat treatment followed by a variety of quenching mediums on the hardness of DSS 2205 are outlined in Table 4. The Vickers micro hardness values for the specimens can range anywhere from 255 to 278 HV, depending on the heating temperature and the varied quenching media used. The greatest effect micro hardness is not demonstrated by the normalizing specimen. The increase in heating temperature and subsequent quick cooling caused a change in the hardness value of the specimens that were heat-treated. As the most important component of the mechanical properties, the average value of hardness was measured on specimens that had not been treated and on those that had been treated, and the results were presented in Figure 4 (at a temperature of 1050 degrees Celsius and using a variety of quenching media). Intermetallic phases, such as the sigma phase, are responsible for the increased hardness that is related with the impact of heat treatment and quenching medium. It was discovered that the intermetallic - sigma phase has a hardness that was significantly higher than that of major phases such as -ferrite or -austenite [14]. The presence or absence of the secondary sigma phase [6, 8, 12] serves as the foundation for the determination of the hardness values. The distortion of the face-cubic crystal structure that results from alternate mixed crystals generated from large grain boundaries components such as Mo, Cr, and N contributes to the hardness of the main -austenite phase [6, 11, 14]. This deformation is the source of the hardness of the main -austenite phase.

In the course of this experiment, none of the specimens, whether they had been treated or left untreated, displayed any signs of secondary phases in their morphologies (see Fig. 3). Because there are no substantial shifts in the

percentage of quantity of phases present in the morphology and because there are no secondary phases, the hardness value that is displayed in Figure 4 does not represent a significant change in harness value. Because of this, the heat treatment is not influenced in this instance. The findings of the hardness test reveal that the normalizing and annealing specimens have different maximum values of hardness. The normalizing specimen has 278 HV as its highest value of hardness.

Table 4. Micro hardness for different quenching medium

Sample	Cooling medium	R1 (HV)	R2 (HV)	R3 (HV)	Average (HV)
A	untreated	259	250	256	255
B	Air cooling	267	258	261	262
C	Water cooling	283	276	275	278
D	Furnace cooling	261	258	260	260

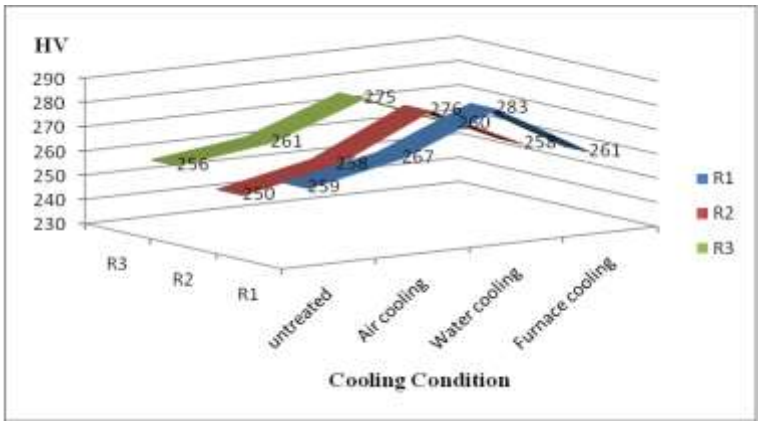

Fig. 4 Variation in micro hardness with cooling condition

5.4 Potentiodynamic polarization:

In Fig. 5, polarization curves for DSS 2205 are displayed to illustrate the effect of high-temperature heat treatment on corrosion performance in 3.5% NaCl solutions representing simulated seawater. Different variables impact corrosion resistance owing to heating temperature, but morphological changes and the production of intermetallic phases have a significant effect in the corrosion performance of DSS alloys [20]. The corrosion resistance of DSS was lowered due to two factors: first, the production of intermetallic phases like sigma, and second, the change in volume proportion of ferrite and austenite, which mostly affected the ferrite phase of DSS [18]. However, Cr is the most effective element in the ferrite phase that increases the corrosion performance of DSS, whereas Ni is the key alloying element in the austenite phase, which has higher corrosion resistance than ferrite. When can be seen in Fig. 5, the current density in the anodic polarization curve rises when the polarization potential is increased. Tafel plots on the potentiodynamic polarization curves shown in Table 5 were used to assess the electrochemical parameters. According to Table 5, the lowest current density (0.80 A/cm2) and highest corrosion resistance (0.360 mpy) are observed in these samples.

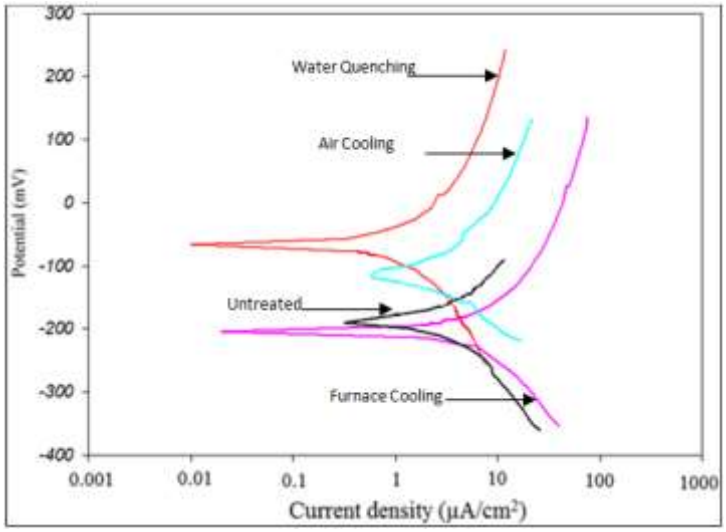

Fig. 5 Polarization curves of DSS 2205 in simulated sea water 3.5 % NaCl solutions

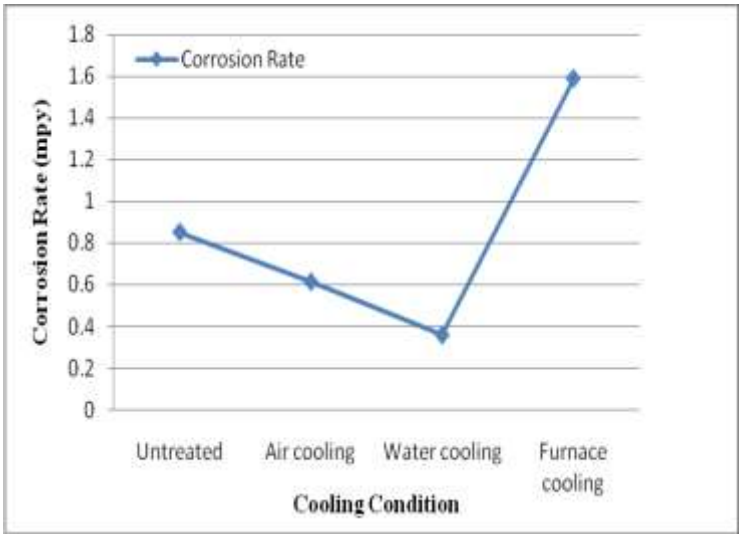

Fig 6. Relation between cooling condition and corrosion rate

Table 5 Data obtained from Potentiodynamic polarization Tafel plot

Heating and cooling condition	E_{corr} (mV)	Current density (µ A/cm^2)	Corrosion rate (mpy)
Untreated	-198	1.99	0.853
1050 °C and air cooling	-123	1.65	0.615
1050 °C and water cooling	-68	0.80	0.360
1050 °C and furnace cooling	-203	3.45	1.589

According to Table 5, the protective potential Ecorr is highest for the water-cooled specimen (-68 mV) and lowest for the furnace-cooled specimen (-203 mV). Fig. 6 depicts the correlation between corrosion rate and cooling condition of specimens. Maximum current density (3.45 A/cm2) and corrosion rate (1.589 mpy) are observed in the furnace

cooled specimen. As the morphology of the specimens changed from one phase to another, the current density decreased from 3.45 to 0.80 A/cm2. Figure 3(3) from the SEM analysis of the water-cooled specimen reveals the best ratio of major phases, with no intermetallic phases present, and a rise in the volume percentage of austenite. This demonstrates that corrosion resistance is morphology-dependent.

5.5 Limitations

When conducting research on the mechanical characteristics, morphology, and corrosion behavior of duplex stainless steel 2205, several limitations may arise. Here are some common limitations:

Limited Availability of Test Specimens: Obtaining an adequate number of test specimens can be challenging, especially if the material is expensive or difficult to manufacture. This limitation may restrict the scope of the research or require collaboration with industry partners to access relevant materials.

Time-Dependent Behavior: Some mechanical and corrosion properties of duplex stainless steel 2205 can exhibit time-dependent behavior, such as creep or stress relaxation. Studying these properties often requires long-duration experiments, which can be time-consuming and may not be feasible within the time constraints of a research project.

Complex Microstructure: Duplex stainless steel 2205 has a complex dual-phase microstructure consisting of austenite and ferrite. Analyzing and characterizing this microstructure accurately can be challenging, especially at high magnifications or when trying to assess local variations. Advanced techniques such as electron microscopy, atom probe tomography, or X-ray diffraction may be necessary, which can be costly or require specialized expertise.

Limited Standardization: Standardization of testing methods and procedures for duplex stainless steel 2205 may be relatively limited compared to other materials. This can make it challenging to compare research results across different studies or establish consistent guidelines for testing and characterization. Researchers may need to rely on established standards for similar materials or develop customized protocols specific to their research.

Environmental Variations: The corrosion behavior of duplex stainless steel 2205 can vary significantly depending on the specific environment in which it is exposed. Conducting research in a controlled and representative environment is crucial, but replicating all possible real-world conditions can be difficult. Researchers should carefully consider the selection and preparation of test environments to ensure relevance and reliability.

Long-Term Durability: Understanding the long-term mechanical and corrosion behavior of duplex stainless steel 2205 is essential for practical applications. However, conducting studies over extended periods can be challenging due to the time and resources required. Accelerated testing methods or extrapolation techniques may be employed to estimate long-term behavior, but these approaches have inherent limitations and may not capture all aspects of real-world performance.

Complexity of Corrosion Mechanisms: Corrosion behavior in duplex stainless steel 2205 can be influenced by various factors, including chemical composition, microstructure, temperature, and environmental conditions. Understanding the specific corrosion mechanisms and their interplay can be complex and requires in-depth analysis. Sophisticated modeling or simulation techniques may be necessary to gain comprehensive insights.

Addressing these limitations often requires careful experimental design, collaboration with experts, access to specialized equipment and facilities, and a thorough understanding of the material's behavior. Despite these challenges, research efforts can contribute significantly to advancing the understanding and utilization of duplex stainless steel 2205 in various applications.

6. Conclusions

The purpose of this research was to determine how different quenching media affected the morphology, impact toughness, micro hardness, and tensile strength of DSS 2205 after being heated to a high temperature of 1050°C. The following are some of the most notable takeaways from the research conducted.

1. One of the most important factors in maintaining a stable percentage volume of phases and preventing the development of intermetallic phases in DSS 2205 is the influence of high temperature heating and varied quenching media.
2. As can be seen from the impact toughness findings, the V-notch specimen has the greatest value of toughness at 33J after normalization.
3. The lack of intermetallic -sigma and -chi phases after heating DSS 2205 to 1050°C had no appreciable effect on micro hardness in any of the cooling settings studied.
4. The micro hardness data demonstrate that the annealed material is up to 278 HV harder than the normalized and untreated specimens.
5. The corrosion data demonstrate that at 1050°C, the water-cooled specimen has the highest corrosion resistance (0.360 mpy) and protective potential (-68 A/cm^2), while the furnace-cooled specimen has the lowest corrosion resistance (1.589 mpy) and protective potential (-203 A/cm^2).
6. Alterations to the cooling environment have resulted in a drop in current density from 3.45 to 0.80 A/cm^2.

References

[1] H. Li, L. Zhang, B. Zhang and Q. Zhang, Effect of heat treatment on the microstructure and corrosion resistance of stainless/carbon steel bimetal plate, *Adv. Mater. Sci. Eng*, (2020), 1–12.

[2] A. Y. Chaudhari & D. D. Deshmukh, Metallurgical investigations on corrosion behavior of simple and heat treated duplex stainless steel 2205 exposed to corrosive media, *IOP Conf. Ser. Mater. Sci. Eng*., 810(1), (2020), p. 012048.

[3] L. Jerzy, A. Swierczyńska and S. Topolska, Effect of microstructure on mechanical properties and corrosion resistance of 2205 duplex stainless steel, *Pol. Marit. Res.* 21 (4), (2016), 108-112.

[4] M. Pan, X. Zhang, P. Chen, X. Su and R. Misra, The effect of chemical composition and annealing condition on the microstructure and tensile properties of a resource-saving duplex stainless steel, *Mater. Sci. Eng. A*, 788, (2020), 139540.

[5] A. S. Hammood, A. F. Noor and M. T. Alkhafagy, Effect of heat treatment on corrosion behavior of duplex stainless steel in orthodontic applications, *Mater. Res. Express.*, 4 (12), (2017), 126506.

[6] M. B. Davanageri, S. Narendranath and R. Kadoli, Influence of Heat Treatment on Microstructure, Hardness and Wear Behavior of Super Duplex Stainless Steel AISI 2507, *Am. J. Mater. Sci.*, 5(3C), (2015), 48-52.

[7] C. Gennari, L. Pezzato, E. Piva, R. Gobbo and I. Calliari, Influence of small amount and different morphology of secondary phases on impact toughness of UNS S32205 Duplex Stainless Steel, *Mater. Sci. Eng. A*, 729, (2018), 149–156.

[8] C. Paulsen, R. Broks, M. Karlsen, J. Hjelen and I. Westermann, Microstructure evolution in super duplex stainless steels containing σ-phase investigated at low-temperature using in situ SEM/EBSD tensile testing, *Metals*, 8(7), (2018), 478.

[9] N. Haghdadi, P. Cizek, P. D. Hodgson and H. Beladi, Microstructure dependence of impact toughness in duplex stainless steels, *Mater. Sci. Eng.*, 745, (2019), 369-378.

[10] G. Argandoña, J. Palacio, C. Berlanga, M. Biezma, P. Rivero, J. Pena and R. Rodriguez, Effect of the temperature in the mechanical properties of austenite, ferrite and sigma phases of duplex stainless steels using hardness, micro hardness and nano indentation techniques, *Metals*, 7(6), (2017), 219.

[11] S. Li, W. Ding, Q. Zhang, X. Xiao and Q. Zhou, Experimental study of the mechanical properties of a new duplex stainless steel exposed to elevated temperatures, *Case Stud. Constr. Mater.*, 17, (2022).

[12] M. Mehta, P. Jadhav, A. Shaikh, S. Kumar and S. Kirwai, Effect of Solution Treatment on Microstructure and Mechanical Properties of 2205 Duplex Stainless Steel, *Int. J. Manuf. Mater. Mech. Eng.*, 7(6), (2019).

[13] Z. Wu, Y. F. Cheng, L. Liu, W. Lu and W. Hu, Effect of heat treatment on microstructure evolution and erosion–corrosion behavior of a nickel–aluminum bronze alloy in Chloride Solution, *Corros. Sci.*, 98, (2015), 260–270.

[14] S. Topolska and J. Labanowski, Impact-toughness investigations of duplex stainless steels, *Mater. Technol.*, 49(4), (2015), 481–486.

[15] D. S. Kahar, Duplex Stainless Steels-an overview, *Int. J. Eng. Res.*, 07 (04), (2017), 27–36.

[16] M. A. Makhdoom, A. Ahmad, M. Kamran, K. Abid and W. Haider, Microstructural and electrochemical behavior of 2205 duplex stainless steel weldments, *Surf Interface Anal.*, 9, (2017), 189–195.

[17] X. Guo, T. Li, Z. Shang, Y. Zhu and G. Li, The precipitation behavior of second phase in high titanium microalloyed steels and its effect on microstructure and properties of steel, *High Temp. Mater. Process.*, 41, (2022), 111-122.

[18] D. D. Deshmukh and V. D. Kalyankar, Deposition characteristics of multitrack overlayby plasma transferred arc welding on ss316lwith co-cr based alloy – influence of process parameters, *High Temp. Mater. Process.*, 38, (2019), 248–263.

[19] K. A. Abdelazem, H. M. El-Aziz, M. M. Ahmed and I. G. El-Batanony, Characterization of mechanical properties and corrosion resistance of SAF 2205 duplex stainless steel groove joints welded using friction stir welding process, *Int J Recent Technol Eng.*, 8(6), (2020), 3428–3435.

[20] V. D. Kalyankar and D. D. Deshmukh, On the performance of metallurgical behaviour of stellite 6 cladding deposited on SS316L substrate with PTAW process, *Can. Metall. Q.*, 61(2), (2022), 130–144.

[21] D. D. Deshmukh and V. D. Kalyankar, Analysis of deposition efficiency and distortion during multitrack overlay by plasma transferred arc welding of Co–CR alloy on 316L Stainless Steel, *J. Adv. Manuf. Syst.*, 20(04), (2021), 705–728.

[22] A. Y. Chaudhari, N. Diwakar and S. D. Kalpande, Effect of heat treatment on microstructure, mechanical and corrosion characteristics of Duplex Stainless Steel 2205: A Review, *scope*, 13 (01), (2023), 301-313.

[23] L. Pezzato, M. Lago, K. Brunelli, M. Breda and I. Calliari, Effect of the heat treatment on the corrosion resistance of Duplex Stainless Steels, *J. Mater. Eng. Perform.*, 27(8), (2018), 3859–3868.